Checkpoint functions are required for normal S-phase progression in *Saccharomyces cerevisiae* RCAF- and CAF-I-defective mutants

Ellen S. Kats, Claudio P. Albuquerque, Huilin Zhou, and Richard D. Kolodner[†]

Ludwig Institute for Cancer Research, Departments of Medicine and Cellular and Molecular Medicine, and Cancer Center, University of California at San Diego School of Medicine, 9500 Gilman Drive, La Jolla, CA 92093-0669

The chromatin-assembly factor I (CAF-I) and the replication-coupling assembly factor (RCAF) complexes function in chromatin assembly during DNA replication and repair and play a role in the maintenance of genome stability. Here, we have investigated their role in checkpoints and S-phase progression. FACS analysis of mutants lacking Asf1 or Cac1 as well as various checkpoint proteins indicated that normal rates of S-phase progression in *asf1* mutants have a strong requirement for replication checkpoint proteins, whereas normal S-phase progression in *cac1* mutants has only a weak requirement for either replication or DNA-damage checkpoint proteins. Furthermore, *asf1* mutants had high levels of Ddc2.GFP foci that were further increased in *asf1 dun1* double mutants consistent with a requirement for checkpoint proteins in S-phase progression in *asf1* mutants, whereas *cac1* mutants had much lower levels of Ddc2.GFP foci that were not increased by a *dun1* mutation. Our data suggest that RCAF defects lead to unstable replication forks that are then stabilized by replication checkpoint proteins, whereas CAF-I defects likely cause different types of DNA damage.

chromatin assembly | DNA-damage response | DNA replication | genome instability

DNA replication and repair require new chromatin assembly, during which the four core histones must be assembled into a histone octamer containing two H2A/H2B dimers and a H3/H4 tetramer wrapped in DNA to form a nucleosome. In the absence of proper chromatin assembly in human cells, DNA synthesis cannot be completed (1, 2). Many histone chaperones are known to be involved in nucleosome and chromatin assembly, of which chromatin assembly factor 1 (CAF-I) and anti-silencing function 1 (Asf1) are among the most studied (reviewed in ref. 3). CAF-I is a nucleosome assembly factor complex that functions during DNA replication and repair and deposits histone H3/H4 tetramers onto DNA (4–7). Asf1 binds histones H3 and H4, forming the replication-coupling assembly factor (RCAF) complex, and is thought to play the role of a histone donor, functioning synergistically with CAF-I (8–11). Among other factors involved in chromatin assembly are NAP-1 (12), which functions as a cytoplasmic-nuclear histone H2A/H2B transfer factor during DNA synthesis, and HIRA (Hir1 and Hir2 in *Saccharomyces cerevisiae*) proteins, which are histone H2A/H2B chaperones that act in the assembly of chromatin independently of DNA synthesis (13, 14).

CAF-I is evolutionarily conserved and in most species contains three subunits. In *S. cerevisiae*, these three subunits are Cac1, Cac2, and Cac3, of which Cac3 directly interacts with histones H3 and H4, and the largest subunit, Cac1, binds proliferating cell nuclear antigen (PCNA) (15). CAF-I facilitates nucleosome assembly preferentially onto newly synthesized DNA (4, 16). In *S. cerevisiae*, deletion of any of the subunits leads to increased UV sensitivity (7) and silencing defects at telomeres as well as at the mating type loci (7, 17, 18). Furthermore, a synergistic decrease in silencing was observed in *S. cerevisiae* cells lacking both CAF-I and Asf1 (8), and there appears to be a synergistic interaction between CAF-I and Asf1 during chromatin assembly linked to DNA replication *in vitro* (10). Consistent with these observations, CAF-I has been shown to physically interact with Asf1 in both human (10) and *Drosophila* (11) cells.

The RCAF complex in *S. cerevisiae* and *Drosophila* consists of the Asf1 histone chaperone protein and histones H3 and H4 (11, 19). As opposed to CAF-I, the RCAF complex cannot promote chromatin assembly coupled to DNA replication on its own; however, it appears to synergize with CAF-I in this role *in vitro* (8, 11). *S. cerevisiae* mutants lacking Asf1 exhibit sensitivity to a wider range of DNA-damaging agents and have a slow growth phenotype compared with CAF-I-defective mutants (8), suggesting that CAF-I and RCAF may have some distinct functions. Asf1 has also been implicated in the buffering of free histones during DNA-damage-induced cell cycle arrest (20) as well as chromatin disassembly at certain loci (21).

Several studies have linked both CAF-I and RCAF to checkpoint regulation. In *S. cerevisiae*, Asf1 and the checkpoint protein Rad53 are known to interact, and Asf1 is dissociated from phosphorylated Rad53 after cells are treated with the DNA damaging agent methyl methane sulfonate (MMS) or hydroxyurea (HU) (22, 23). However, a recent analysis of physiological levels of Asf1 has indicated that Asf1 can interact with phosphorylated Rad53 in response to MMS (24). In humans and *Drosophila*, Asf1 has also been implicated in checkpoint related signaling due to being the only known substrate for Tlk (tousled-like kinase), which is inhibited by the ATM/Chk1 DNA-damage-checkpoint pathway (25, 26). Furthermore, *asf1* mutant cells have been previously shown to be partially defective in HU-induced Rad53 phosphorylation (22), suggesting that *asf1* mutants may be partially checkpoint-defective. Consistent with this idea, the apparent inability of *asf1* mutants to recover from HU arrest as suggested by FACS (8) is similar to the behavior of mutants that have a defect in the replication checkpoint (27). In addition, expression of a dominant-negative Cac1 protein, the largest component of CAF-I, has been shown to cause DNA damage and activate the S-phase checkpoint in human cells (2). In our previous work, we showed that mutations in the genes encoding the CAF-I and RCAF complexes caused increased rates of accumulation of gross chromosomal rearrangements in *S. cerevisiae* (28). Our genetic analysis suggested that Asf1 defects could result in DNA damage that activated both the replication and DNA-damage checkpoints, whereas CAF-I defects might result in activation of the DNA-damage checkpoint. Consistent with this, a recent study has demonstrated activation of the DNA-damage checkpoint in an *asf1* mutant (29).

In the present study, we have investigated whether RCAF and CAF-I play a role in checkpoint regulation. Our results show that
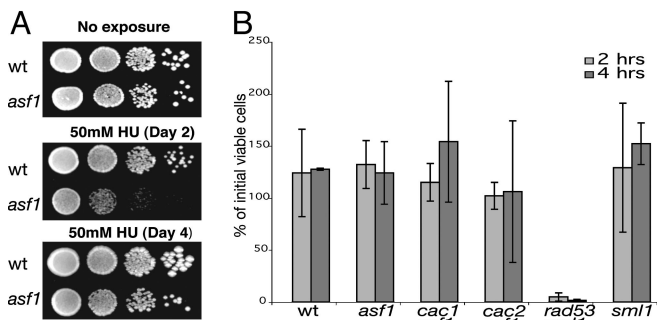

Fig. 1. *asf1* mutants are not killed by either chronic or acute HU treatment. (*A*) Cells were plated on YPD and 50 mM HU plates and incubated at 30°C, as indicated. (*B*) Cell survival after acute treatment of cells with 200 mM HU for 2- or 4-h periods is shown as the percent of viable cells present before treatment.

Fig. 2. *asf1 caf-1* double mutants exhibit a higher proportion of cells in G$_2$/M and accumulate aberrant buds indicative of DNA damage. (*A*) Log-phase cells were stained with DAPI and analyzed by fluorescent microscopy. Each strain was scored for the percentage of cells with no buds, small buds, large buds, and aberrant buds. The distribution for CAF-I mutants, in the order stated above, were *cac1* (18%, 48%, 30%, and 4%), *cac2* (19%, 48%, 29%, and 3%), and *cac3* (15%, 55%, 28%, and 2%). (*B*) The DNA content of the same series of mutants was determined by FACS analysis of cells from log-phase unsynchronized cultures.

defects in these chromatin assembly factors do not cause checkpoint defects. In contrast, *asf1* mutants were found to depend highly on the S-phase checkpoints for normal progression through S phase. Furthermore, cells that are defective for both CAF-I and RCAF appear to have increased S-phase progression defects resulting in the accumulation of cells arrested in G$_2$/M consistent with the accumulation of DNA damage during S phase. These results are interpreted in terms of models in which RCAF mutants are partially defective in maintaining replication fork structure and that this defect is exacerbated by both checkpoint and CAF-I defects.

Results

asf1 Mutants Are Sensitive to Killing by MMS but Not HU.
Many checkpoint-defective mutants, such as a *rad53Δ* mutant, are sensitive to killing by both HU and MMS. We therefore tested all possible single, double, and triple combinations of CAF-I subunit mutations, none of which caused sensitivity to either 50 mM HU or 0.01% or 0.02% MMS (Fig. 7, which is published as supporting information on the PNAS web site) (data not shown); note that in an S288c strain (our background) CAF-I defects did not cause sensitivity to 0.02% MMS, whereas in a W303 strain sensitivity to 0.02% MMS was seen (30). In contrast, the *asf1* single mutant and the *cac1 asf1*, *cac2 asf1*, and *cac3 asf1* double mutants were all sensitive to killing by MMS (Fig. 8, which is published as supporting information on the PNAS web site). The *asf1* single mutant and the *cac1 asf1*, *cac2 asf1*, and *cac3 asf1* double mutants appeared to be sensitive to killing by HU when the plates were incubated at 30°C for up to 3 days, but upon longer incubation all four mutant strains exhibited wild-type levels of survival (Fig. 1*A*) (data not shown). Thus, these mutants appear to grow much more slowly in the presence of HU but are not killed.

Mutants that are defective for the replication checkpoint cannot recover from acute treatment with concentrations of HU (200 mM) that result in depletion of nucleotide pools and subsequent DNA replication arrest. Consistent with this, the checkpoint-defective *rad53 sml1* mutant was unable to recover from either 2- or 4-h treatment with HU. In contrast, the *asf1* single mutant and the *cac1 asf1*, *cac2 asf1*, and *cac3 asf1* double mutants all showed the same full recovery as the wild-type and *sml1* single mutant control strains (Fig. 1*B*). This result confirms that the *asf1* single mutant and the *cac1 asf1*, *cac2 asf1*, and *cac3 asf1* double mutants are not sensitive to killing by HU.

Analysis of Cell Morphology Suggests That RCAF Single Mutants and RCAF CAF-I Double Mutants Have a Cell Cycle Progression Defect.
The *asf1* single mutant and the *cac1 asf1*, *cac2 asf1*, and *cac3 asf1* double mutants all appear to have a modest reduction in growth rate compared with wild-type control strains or *cac1*, *cac2*, or *cac3* single mutants. To better understand this, the morphology of cells from
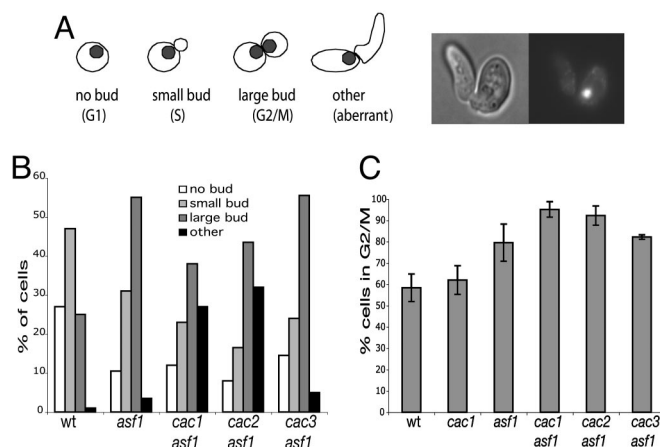
log-phase cultures of these mutants and control strains were analyzed by fluorescence microscopy (Fig. 2 *A* and *B*). The largest class of wild-type cells had small buds and a single nucleus, and thus appeared to be in early S phase. The *cac1*, *cac2*, and *cac3* single mutants were all similar to wild-type cells (see legend of Fig. 2). Compared with the wild-type strain, *asf1* mutants had a large increase in the number of large-budded cells along with a decrease in the proportion of cells with either no bud and a single nucleus or a small bud and a single nucleus; the *cac3 asf1* double mutant showed a distribution of cells that was similar to that of the *asf1* mutant. Likewise, in comparison with the wild-type cells, the *cac1 asf1* and *cac2 asf1* double mutants showed an increase in large-budded cells with DNA staining in both buds along with a decrease in the proportion of cells with either no bud and a single nucleus or a small bud and a single nucleus. However, in contrast to *asf1* mutants, these two mutants exhibited a large increase in the number of cells having aberrant bud morphologies in which buds were elongated and misshapen, with a single nucleus at the bud neck (Fig. 2*A*).

Analysis of the G$_2$/M DNA content in the same cultures by FACS was consistent with the cell morphology analysis (summarized in Fig. 2*C*). One interpretation of the FACS results in combination with the cell morphology analysis is that the *asf1* single and double mutant cells are accumulating DNA damage during DNA replication resulting in slower progression through the G$_2$/M phase of the cell cycle, whereas this may not be the case with CAF-I single mutants.

Chromatin Assembly Mutants Are Proficient for the Replication and Intra-S Checkpoints.
There appeared to still be some question as to whether *asf1* mutants are checkpoint-defective (31), leading us to further study the replication and intra-S checkpoint proficiency of chromatin assembly mutants. We examined chromatin assembly mutants, as well as appropriate controls, by FACS to monitor their ability to resume the cell cycle after arrest with 200 mM HU. We found that all of the chromatin assembly mutants showed the same kinetics and extent of recovery from HU arrest as the wild-type control (Fig. 9, which is published as supporting information on the PNAS web site). Intra-S checkpoint proficiency was examined by releasing α-factor arrested cells into 0.03% MMS and observing the ability of mutant and control cells to sense the DNA damage,
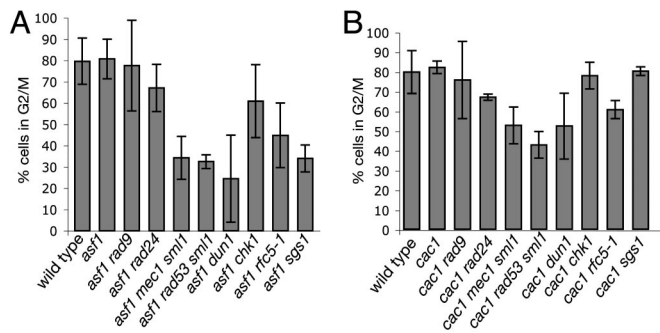
Fig. 3. *asf1* and *cac1* mutants require the function of different checkpoints for normal S-phase progression. FACS was used to monitor the rate of S-phase progression of various chromatin assembly/checkpoint double mutants after release from α-factor arrest. The proportion of cells in G$_2$/M was determined at the 40-min time point, at which at least 80% of wild-type cells have reached G$_2$/M. Error bars represent the SD. The percent of cells in G$_2$/M for the control strains was as follows: *rad9*, 81 ± 4%; *rad24*, 86 ± 6%; *mec1 sml1*, 85 ± 5%; *rad53 sml1*, 81 ± 4%; *dun1*, 80 ± 2%; *chk1*, 82 ± 10%; *rfc5-1*, 74 ± 7%; *sgs1*, 83 ± 7%.

demonstrated by significant slowing of S-phase progression. Again, all of the chromatin assembly mutants behaved like the wild-type control (Fig. 10, which is published as supporting information on the PNAS web site). Thus, these mutants have fully functional replication and intra-S checkpoints.

S-Phase Progression in *asf1* Mutants Depends on Functional Checkpoints. We have previously suggested that defects in the genes encoding CAF-I appear to cause some type of DNA damage that is processed by the DNA-damage checkpoints, whereas a defect in the *ASF1* gene causes some type of DNA damage that is processed by both the DNA-damage and the replication checkpoints (28). Therefore, it was of interest to determine whether inactivation of different checkpoints has an effect on S-phase progression in these chromatin assembly mutants. We monitored S-phase progression of *asf1* and *cac1* mutants containing mutations that inactivate DNA-damage and intra-S DNA-damage checkpoint sensors (*rad24* and *rad9*), replication checkpoint sensors (*rfc5-1* and *dpb11-1*), replication and intra-S checkpoint sensors (*sgs1*), and checkpoint transducers (*mec1*, *rad53*, *dun1*, and *chk1*) after release from G$_1$ arrest (31, 32). The rate of progression through S phase was evaluated by determining the proportion of cells that accumulated in G$_2$/M phase at 40 min after release from α-factor arrest (Fig. 3).

Despite initiating S phase slightly later than wild-type cells and growing slightly slower, *asf1* mutants accumulated the same proportion of cells in G$_2$/M by 40 min after release as the wild-type cells (81% vs. 80%). The *asf1 rad9* and *asf1 rad24* mutants did not demonstrate a significant S-phase progression delay compared with wild-type cells or *asf1* mutants as evidenced by their proportion of G$_2$/M cell cells at 40 min (78% and 67%, respectively). In contrast, the *asf1 dun1*, *asf1 mec1 sml1*, *asf1 rad53 sml1*, and *asf1 sgs1* mutants exhibited a significant delay in S-phase progression (24%, 34%, 32%, and 34% G$_2$/M cells at 40 min, respectively) and also had a higher proportion of S-phase cells at this time point. The *asf1 rfc5-1* mutants also showed a reproducible decrease in G$_2$/M content cells (45%), although not as large as in *asf1 dun1*, *asf1 mec1 sml1*, *asf1 rad53 sml1*, and *asf1 sgs1* mutants. It was not possible to analyze the *asf1 dbp11-1* double mutant because it had a severe growth defect (data not shown). Unlike *asf1 dun1* or *asf1 rad53 sml1* mutants, the *asf1 chk1* mutant did not appear to exhibit a significant S-phase delay (61%). Cells with a *cac1* mutation did not appear to exhibit slowed progression through S phase and had an average G$_2$/M content of 80% of the cells at 40 min after α-factor release (Fig. 3B). The *rad9*, *rad24*, *rfc5-1*, and *sgs1* mutations did not appear to cause a significant slowing of S-phase progression in a *cac1* mutant.

However, *cac1 mec1 sml1*, *cac1 dun1*, and *cac1 rad53 sml1* mutants did appear to show a small but significant reduction in S-phase progression (53%, 52%, and 43% G$_2$/M cells at 40 min, respectively) as compared with the *cac1* single mutant.

The analysis presented here indicates that *asf1* and *cac1* mutations cause different effects in the S-phase progression assay. The data are consistent with the idea that *asf1* mutants depend on replication checkpoint proteins to transit S phase, as evidenced by the S-phase progression phenotype of the *asf1 rfc5-1*, *asf1 mec1 sml1*, *asf1 dun1*, *asf1 rad53 sml1*, and *asf1 sgs1* mutants and the lack of a slowed phenotype of the *asf1 rad9* and *asf1 rad24* mutants. In contrast, *cac1* mutants show little if any checkpoint protein dependence for progression through S phase as evidenced by the weak phenotypes seen only with the *cac1 mec1 sml1*, *cac1 rad53 sml1*, and *cac1 dun1* mutants.

Analysis of Spontaneous Checkpoint Protein Assembly in *asf1* and *cac1* Mutants. Previously published results showing that both *asf1* and *cac1* mutants have elevated levels of gross chromosomal rearrangements and that *asf1* and *cac1* mutations showed synergistic interactions with different checkpoint defects (28) raised the hypothesis that chromatin assembly mutants accumulate DNA damage that activates checkpoints during replication. The findings presented here that *asf1* mutants, and to a small extent *cac1* mutants, depend on checkpoint proteins for normal S-phase progression is consistent with this idea. To further investigate this hypothesis, we examined the formation of DNA-damage foci in log-phase cultures of key mutant strains using a functional GFP-tagged version of the Ddc2 protein (Fig. 4). Ddc2 is recruited to sites of DNA damage during checkpoint activation (33); thus, formation of Ddc2.GFP foci is indicative of endogenous DNA damage being sensed by the checkpoint machinery.

We found that in the wild-type strain, 8% of the cells had Ddc2.GFP foci, consistent with previously published results (33). There was a slight, but significant, increase in the *cac1* mutant cells, with 15% containing Ddc2.GFP foci (Fig. 4C). In contrast, *asf1* mutants exhibited an ≈4-fold increase over wild-type cells, with 33% of cells containing Ddc2.GFP foci (Fig. 4B), similar to a recent study (29). The Ddc2.GFP foci were only seen in budding cells. These data suggest that there are varying degrees of endogenous DNA damage in *asf1* and *cac1* mutant cells, and this could explain the dependency of S-phase progression on the Mec1–Rad53–Dun1 pathway. Interestingly, the *cac1 asf1* double mutant had a similar proportion of cells with Ddc2.GFP foci (14%) to that seen in a *cac1* mutant (Fig. 4C), despite exhibiting a more severe growth phenotype than either of the single mutants, suggesting that the growth and morphological defects in *cac1 asf1* mutants may not be due to replication defects.

We also examined Ddc2.GFP foci formation in both the *asf1 dun1* and *cac1 dun1* mutants. A *dun1* mutation would be expected to inactivate the checkpoint downstream from assembly of Ddc2.GFP foci, allowing us to monitor checkpoint activation in the absence of checkpoint execution (31, 34, 35). We found a significant increase in Ddc2.GFP foci in *asf1 dun1* mutants, with 45% of cells containing one or more Ddc2.GFP focus (Fig. 4B). In contrast, the *cac1 dun1* cells exhibited a smaller, but significant increase in damage foci formation compared with the *cac1* single mutant, with 17% of cells containing Ddc2.GFP foci (Fig. 4C). These findings are consistent with the results of the FACS experiments suggesting that *asf1* mutants, more so than *cac1* mutants, require Mec1–Rad53–Dun1 checkpoint pathway proteins for progression through S phase. These findings also support the view that in the absence of a functional checkpoint, chromatin assembly mutants, especially *asf1* mutants, have an exacerbated S-phase progression defect that results in increased levels of Ddc2 foci.

We also examined the formation of Ddc2.GFP foci in *asf1 rad9* and *cac1 rad9* cells. If *asf1* or *cac1* mutants indeed activated a Rad9 DNA-damage checkpoint, then it is possible that in the absence of
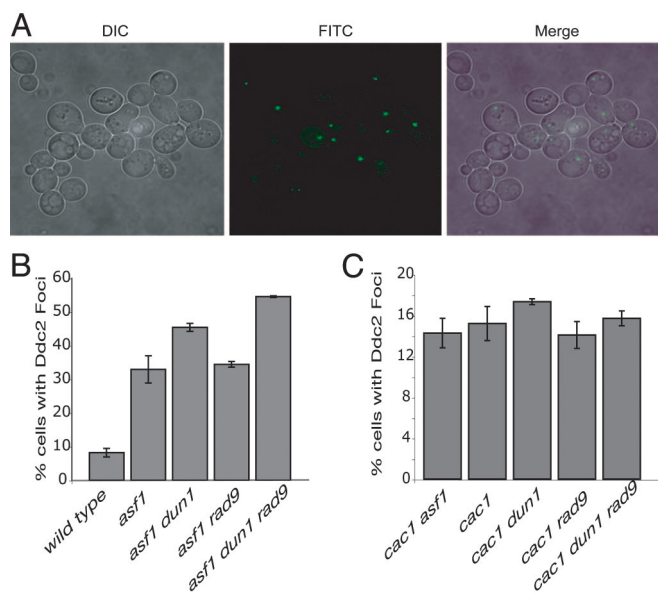
Kats *et al.*

Fig. 4. Ddc2.GFP checkpoint protein complexes accumulate in *asf1* and *cac1* mutants. Live cells were analyzed in log phase by deconvolution microscopy to visualize Ddc2.GFP expression from an endogenous functional *DDC2.GFP* fusion gene resulting in Ddc2.GFP foci. (*A*) Cells are shown in *Left* (DIC), GFP fluorescence is shown in *Center* (FITC), and the two images are merged in *Right* (Merge). The experimental results quantified for *asf1* (*B*) and *cac1* (*C*) mutant cells are expressed as the percentage of cells containing Ddc2.GFP foci. The error bars presented are SDs. The control mutants *rad9 DDC2.GFP* and *dun1 DDC2.GFP* had 13% and 7% cells with Ddc2.GFP foci, respectively.

a Rad9 pathway *asf1* and *cac1* mutants would accumulate more damage resulting in more recruitment of Ddc2 to DNA. However, consistent with the FACS analysis, there was no increase in Ddc2.GFP foci formation in either *asf1 rad9* (34%) or *cac1 rad9* (14%) mutants (Fig. 4 *B* and *C*). Interestingly, the *asf1 dun1 rad9* triple mutant had a modestly higher proportion of cells with Ddc2-GFP foci (55%) compared with both the *asf1* and *asf1 dun1* mutants. In contrast, the *cac1 dun1 rad9* triple mutant did not have an increased proportion of cells with Ddc2.GFP foci (15%) compared with either the *cac1* or *cac1 dun1* mutants. These data support the view that *asf1* defects primarily result in a requirement for replication checkpoint proteins, in the absence of which a secondary requirement for the DNA-damage checkpoint might occur. In contrast, *cac1* defects cause little requirement for checkpoint proteins.

Analysis of Spontaneous Rad53 Phosphorylation in *asf1* and *cac1* Mutants. To confirm the results obtained by examining Ddc2.GFP foci formation, we evaluated checkpoint activation by monitoring Rad53 phosphorylation using quantitative mass spectrometry (24). The relative abundance of both unphosphorylated peptides and phosphopeptides of Rad53 purified from wild-type cells and either *cac1* or *asf1* cells was quantified by stable isotope labeling and mass spectrometry. As shown in Tables 1 and 2 (which are published as supporting information on the PNAS web site), the relative abundance of Rad53 in wild-type, *cac1* and *asf1* cells was similar, as measured by quantitative analysis of multiple unphosphorylated peptides.

We next identified and quantified the relative abundance of phosphopeptides of Rad53 in wild-type and *cac1* cells. Five different phosphopeptides were found (see Table 3, which is published as supporting information on the PNAS web site), representing both proline-directed and non-proline-directed phosphorylation of Rad53. As shown previously (24), the non-proline-directed phosphorylation is due to autophosphorylation of Rad53, which accom-
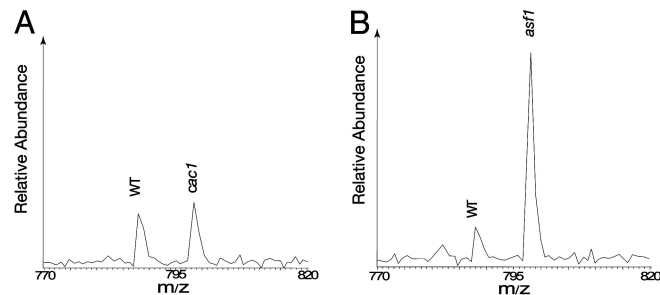

Fig. 5. Levels of Rad53 phosphorylation in *cac1* and *asf1* cells compared with that in wild-type cells. A phosphopeptide (LLHS*NNTENVK; the asterisk indicates the phosphorylated Ser to its right, i.e., Ser-560) of Rad53 is used as an example. (*A*) The abundance of this phosphopeptide was unaffected by deletion of *CAC1*. (*B*) The abundance of this phosphopeptide increased to almost 5-fold in *asf1* cells, compared with wild-type cells. In both cases, Rad53 peptides from wild-type cells were labeled by d0-leucine, whereas those from *cac1* or *asf1* cells were labeled by d10-leucine.

panies its activation. The detection of the autophosphorylation of Rad53 is not unexpected and it indicates a basal level of Rad53 activation in the unperturbed cells. Comparison of the phosphopeptides of Rad53 between wild-type and *cac1* cells shows that there was little change in their abundance (Table 3). As an example, a phosphopeptide of Rad53 (LLHS*NNTENVK), containing phosphorylation of Ser-560, is shown in Fig. 5*A*. Phosphorylation of Ser-560 is an autophosphorylation event that serves as an indicator for Rad53 activation, demonstrating that there was no detectable change in the activation of Rad53 in the *cac1* mutants.

In contrast, when the phosphopeptides of Rad53 in *asf1* cells were compared with those in wild-type cells, the non-proline-directed autophosphorylation of Rad53 was clearly enhanced. As shown in Fig. 5*B*, the level of phosphorylation of Ser-560 in *asf1* mutants was almost 5-fold higher than that in wild-type cells. Similarly, phosphorylation of Ser-789, an initial event in Rad53 autophosphorylation, and phosphorylation of Ser-747–748 and Ser-774 were also more abundant in *asf1* cells (see Table 4, which is published as supporting information on the PNAS web site). Previous analysis of MMS-treated wild-type cells identified many more autophosphorylation sites of Rad53 with a much higher level of induction (24) than seen here in *asf1* mutants. Thus, the level of Rad53 activation resulting from deletion of *ASF1* appears to be higher than in wild-type cells but below the levels of a full checkpoint response, which is consistent with Western blot analysis of Rad53 phosphorylation in *asf1* mutants (22, 29).

Discussion

In the present study, we have examined the genetic interplay between the RCAF and CAF-I chromatin assembly factors and different checkpoints. Our results demonstrate that defects in the genes encoding the RCAF and CAF-I complexes do not cause defects in the replication or intra-S DNA-damage checkpoints. We further found that normal progression of *asf1* mutants through S phase depended on replication checkpoint proteins, whereas S-phase progression of CAF-I-defective mutants only weakly depended on checkpoint proteins. Consistent with these checkpoint protein requirements, *asf1* mutants exhibited increased levels of Ddc2.GFP foci, which were further increased when checkpoint function was inactivated downstream of Ddc2 by a *dun1* mutation. In contrast, CAF-I-defective mutants exhibited a much smaller increase in Ddc2.GFP foci in these assays. However, quantitative analysis of Rad53 phosphorylation indicated that *asf1* mutants showed only low levels of spontaneous checkpoint activation similar to previous results (22, 29), and *cac1* mutants did not show any checkpoint activation. The fact that a *rad9* mutation did not increase the level of Ddc2.GFP foci in *asf1* mutants and that *rad9* and *rad24*
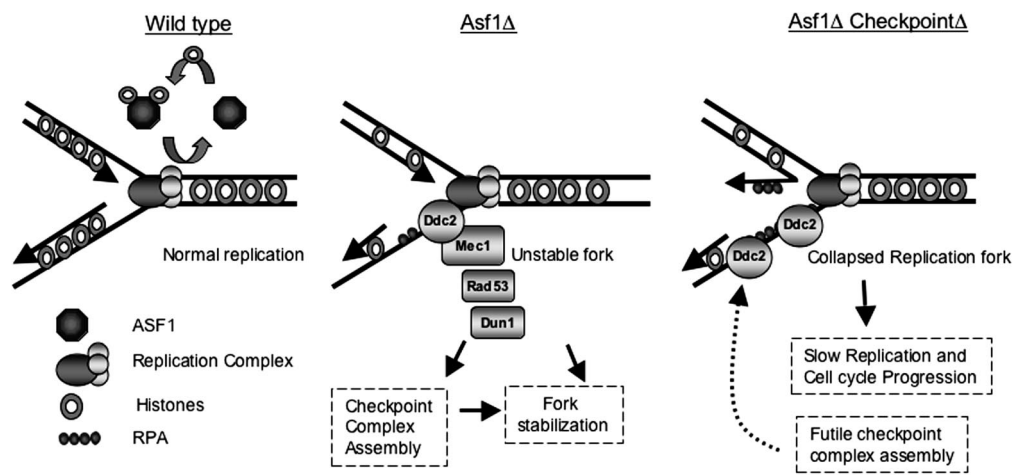
Fig. 6. A model for the role of Asf1 in DNA replication and checkpoint activation. Asf1 plays an important role at replication forks during replication and repair. In the absence of Asf1, replication forks become unstable, leading to slower progression through S phase. Although somewhat unstable, these replication forks remain functional because of the presence of various replication checkpoint proteins, such as Ddc2, Rad53, and others, which play roles in replication forks stabilization. In the absence of a functional replication checkpoint, these somewhat unstable replication forks may collapse, thus leading to even slower S-phase progression, as well as conversion of the replication forks into structures that activate the DNA-damage checkpoint.

mutations did not affect the rate of S-phase progression in an *asf1* mutant again points to a role for replication, rather than damage checkpoint proteins, in the stabilization of damaged DNA structures that may arise in *asf1* mutants. Finally, although CAF-I defects did not cause a cell cycle progression defect, RCAF CAF-I double mutants showed a more severe cell cycle progression defect with lower levels of Ddc2.GFP foci than that seen in an *asf1* mutant.

Initial studies indicated that RCAF functions in the assembly of chromatin during DNA replication, although subsequent studies have implicated RCAF in additional processes including disassembly of chromatin and assembly of selected replication factors at replication forks (3, 36, 37). A model interpreting the results of our analysis of *asf1* mutants, as well as prior results, is presented in Fig. 6. We propose that in the absence of Asf1, replication forks are somewhat unstable, explaining the observation that *asf1* mutants appear to enter S phase slightly later and progress through S phase slightly more slowly than wild-type cells. Fork instability could result from a deficit of histones on newly replicated DNA near replication forks, a lack of chromatin remodeling by the Asf1 chromatin disassembly function during DNA replication, or decreased assembly of replication factors at replication forks (21, 37, 38). However, these modestly unstable replication forks are primarily stabilized by proteins that function in the replication checkpoint and not the damage checkpoints (39, 40). Because a number of replication checkpoint proteins are known to be normal components of the replication machinery (reviewed in ref. 31), stabilization could be mediated either directly by assembly of these proteins at replication forks or through checkpoint activation implied by the observed increase in Ddc2.GFP foci when Dun1 is inactivated in an *asf1* mutant. These mechanisms would explain the much slower S-phase progression and synergistic increase in genomic instability of mutants defective for both Asf1 and the replication checkpoint as well as the increased assembly of checkpoint protein foci in *asf1* mutants containing downstream checkpoint defects (28). Although the DNA-damage checkpoint proteins appear to play little role in S-phase progression of *asf1* mutants, the increase in Ddc2.GFP foci in the *asf1 dun1 rad9* triple mutant could reflect a possible conversion of replicating DNA in the *asf1 dun1* double mutant into structures that activate the DNA-damage checkpoint.

It has been suggested that RCAF and CAF-I function in the same chromatin assembly process (8, 11), leading us to perform parallel analyses of RCAF and CAF-I defects in the present study. Consistent with other studies indicating that RCAF and CAF-I have at least some distinct cellular roles (36, 41), we observed that defects in CAF-I did not cause the same effects on HU or MMS sensitivity, S-phase progression, Ddc2.GFP foci formation, or checkpoint

activation as caused by an *asf1* mutation. The aberrant bud phenotype seen in *cac1 asf1* and *cac2 asf1* double mutants is particularly interesting in that it correlates with a strong growth defect which is much more severe than in the respective single mutants. Furthermore, the double mutants are similar to *asf1* single mutants in regard to S-phase progression and damaging agent sensitivity and similar to *cac1* single mutants in regard to Ddc2.GFP foci phenotypes. Interestingly, the *cac3 asf1* double mutant does not show either the increased aberrant bud or the slow growth phenotype, suggesting that these *cac1 asf1* and *cac2 asf1* phenotypes may be independent of histone deposition defects. It is tempting to speculate that these *cac1 asf1* and *cac2 asf1* defects are due to a defect in cell division and budding rather than DNA replication and chromatin assembly. Consistent with this, CAF-I has been implicated in kinetochore maintenance (42, 43) and has recently been linked to the control of the anaphase-promoting complex (APC) (41), a process thought not to involve Cac3. Given this, it is possible that *cac1*- and *cac2*-specific DNA damage leading to genome instability is the result of errors occurring during cell division, such as chromosome mis-segregation due to inappropriate kinetochore assembly, rather than errors occurring during DNA replication. This might explain the high gross chromosomal rearrangement rate seen in *cac1* mutants even though *cac1* mutants do not accumulate high levels of Ddc2.GFP.

This study identifies differences between the RCAF and CAF-I complexes *in vivo*, providing further evidence that although both complexes act as histone chaperones for histones H3 and H4, their functions during DNA replication and cell division may be quite different. Although further work is needed to investigate whether the high gross chromosomal rearrangement rates and low levels of checkpoint complex assembly in *cac1* mutants actually reflect a role for CAF-I during cell division, it is apparent that Asf1 plays a critical role during DNA replication, specifically at replication forks. Future experiments will be required to investigate the role of Asf1 in replication fork stabilization and progression.

Materials and Methods

Strains and Media. *S. cerevisiae* strains were grown in yeast extract/peptone/dextrose (YPD) medium or synthetic complete medium lacking the appropriate amino acid. G418 resistant colonies were selected on YPD plates containing 200 mg/liter geneticin. All of the strains used were derived from the S288c strain RDKY3615 (*MAT*a, *ura3-52*, *leu2Δ1*, *trp1Δ63*, *his3Δ200*, *lys2ΔBgl*, *hom3-10*, *ade2Δ1*, *ade8*, *hxt13::URA3*) by either crossing with other RDKY3615 derivatives or by standard gene disruptions. The RDKY5764 strain background (*MAT*a, *ura3-52*, *trp1Δ63*, *his3Δ200*, *DDC2.GFP*) used for analysis of Ddc2.GFP foci was created by

Kristina S. Schmidt (Ludwig Institute for Cancer Research); it was derived from the same S288c parent strain as RDKY3615. The detailed genotypes of these strains are listed in Table 5, which is published as supporting information on the PNAS web site.

Sensitivity to HU and MMS. Cells were grown in YPD medium to log phase. Serial dilutions were made and spotted onto previously prepared sensitivity plates (50 mM HU, 0.01% MMS, and 0.02% MMS) and grown for 2 (or more, as indicated) days at 30°C.

HU-Survival Assay. Cells were first grown to log phase in YPD, and serial dilutions of the culture were plated onto YPD plates to determine the concentration of viable cells. HU was then added to the culture at a final concentration of 200 mM for periods of 2 and 4 h, after which serial dilutions of the cultures were plated onto YPD plates. The plates were incubated for 2–3 days at 30°C. Survival was calculated by determining the percentage of viable cells present after HU treatment compared with the untreated culture. These experiments were performed in triplicate.

α-Factor Arrest. Cells were grown in YPD medium to log phase. α-factor (Sigma) was added to the culture at a concentration of 5 μg/ml. The culture was then incubated for 2 h at 30°C with shaking, and arrest was monitored by phase-contrast light microscopy. The cells were then pelleted, washed with water, and resuspended in fresh YPD.

FACS Analysis. Cells were fixed in 70% ethanol for 1 h at room temperature, harvested by centrifugation, and resuspended in 50 mM sodium citrate buffer (pH 7.0). After sonication and centrifugation, the cells were once again resuspended in sodium citrate buffer and treated with 250 μg/ml RNase A (United States Biochemical) and 1 mg/ml proteinase K (Sigma) overnight at 37°C. The cells were then harvested by centrifugation, resuspended in 1 ml of sodium citrate buffer containing 1 μM Sytox Green (Molecular Probes), and incubated at room temperature for 2 h. Samples were analyzed by using a FACSVantage SE machine (BD Immunocytometry Systems).

Calculating G$_2$/M Content of Cells. FACS profiles were analyzed by using WINMDI 2.8 software (http://facs.scripps.edu). G$_2$/M content was calculated by measuring the number of events in the later half of the 2N DNA content peaks. This number was then multiplied by 2 and expressed as the percentage of the total of gated events. Experiments were performed in duplicate.

Quantitation of Bud Morphology. Cells were grown in YPD medium to log phase, sonicated, stained with DAPI, and examined by fluorescence microscopy. Four hundred to 600 cells were counted for each mutant. Experiments were done in duplicate, and the percentage of cells in indicated morphology classes was determined.

Quantitation of Ddc2.GFP Foci. Cells were grown in YPD medium to log phase and examined live by using a DeltaVision Restoration confocal microscope (Applied Precision). Images were collected in 0.2-μm z-sections to allow viewing of the entire content of the cells. Two hundred to 300 cells were imaged and counted for each experiment. SOFTWORX software (Applied Precision) was used for image analysis. Experiments were done in duplicate.

Determination of Rad53 Phosphorylation by Mass Spectrometry. Purification of Rad53-TAP in wild-type, *cac1*, and *asf1* background cells was performed as described in ref. 24. The purified Rad53 was digested by trypsin and labeled by an N-isotag reagent with d0- or d10-leucine, instead of d0- or d6-γ-amino butyric acid (GABA). There is no difference in protein quantification when using different amino acid based N-isotag reagents (unpublished observations). Leucine is used here because of its simplicity in synthesis, and the d0 form is commercially available. Boc-d0-Leu-NHS was purchased from NovaBiochem, and Boc-d10-Leu-NHS was synthesized from d10-leucine (Sigma-Aldrich), using the same protocol as for synthesis of Boc-d6-GABA-NHS (24). Mass spectrometry analysis and protein quantification were performed as described in ref. 24.

1. Nelson, D. M., Ye, X., Hall, C., Santos, H., Ma, T., Kao, G. D., Yen, T. J., Harper, J. W. & Adams, P. D. (2002) *Mol. Cell. Biol.* **22,** 7459–7472.
2. Ye, X., Franco, A. A., Santos, H., Nelson, D. M., Kaufman, P. D. & Adams, P. D. (2003) *Mol. Cell* **11,** 341–351.
3. Loyola, A. & Almouzni, G. (2004) *Biochim. Biophys. Acta* **1677,** 3–11.
4. Smith, S. & Stillman, B. (1989) *Cell* **58,** 15–25.
5. Gaillard, P. H., Martini, E. M., Kaufman, P. D., Stillman, B., Moustacchi, E. & Almouzni, G. (1996) *Cell* **86,** 887–896.
6. Kamakaka, R. T., Bulger, M., Kaufman, P. D., Stillman, B. & Kadonaga, J. T. (1996) *Mol. Cell. Biol.* **16,** 810–817.
7. Kaufman, P. D., Kobayashi, R. & Stillman, B. (1997) *Genes Dev.* **11,** 345–357.
8. Tyler, J. K., Adams, C. R., Chen, S. R., Kobayashi, R., Kamakaka, R. T. & Kadonaga, J. T. (1999) *Nature* **402,** 555–560.
9. Sharp, J. A., Fouts, E. T., Krawitz, D. C. & Kaufman, P. D. (2001) *Curr. Biol.* **11,** 463–473.
10. Mello, J. A., Sillje, H. H., Roche, D. M., Kirschner, D. B., Nigg, E. A. & Almouzni, G. (2002) *EMBO Rep.* **3,** 329–334.
11. Tyler, J. K., Collins, K. A., Prasad-Sinha, J., Amiott, E., Bulger, M., Harte, P. J., Kobayashi, R. & Kadonaga, J. T. (2001) *Mol. Cell. Biol.* **21,** 6574–6584.
12. Ishimi, Y., Hirosumi, J., Sato, W., Sugasawa, K., Yokota, S., Hanaoka, F. & Yamada, M. (1984) *Eur. J. Biochem.* **142,** 431–439.
13. Mosammaparast, N., Ewart, C. S. & Pemberton, L. F. (2002) *EMBO J.* **21,** 6527–6538.
14. Park, Y. J., Chodaparambil, J. V., Bao, Y., McBryant, S. J. & Luger, K. (2005) *J. Biol. Chem.* **280,** 1817–1825.
15. Zhang, Z., Shibahara, K. & Stillman, B. (2000) *Nature* **408,** 221–225.
16. Verreault, A., Kaufman, P. D., Kobayashi, R. & Stillman, B. (1996) *Cell* **87,** 95–104.
17. Enomoto, S., McCune-Zierath, P. D., Gerami-Nejad, M., Sanders, M. A. & Berman, J. (1997) *Genes Dev.* **11,** 358–370.
18. Enomoto, S. & Berman, J. (1998) *Genes Dev.* **12,** 219–232.
19. Le, S., Davis, C., Konopka, J. B. & Sternglanz, R. (1997) *Yeast* **13,** 1029–1042.
20. Groth, A., Ray-Gallet, D., Quivy, J. P., Lukas, J., Bartek, J. & Almouzni, G. (2005) *Mol. Cell* **17,** 301–311.
21. Adkins, M. W., Howar, S. R. & Tyler, J. K. (2004) *Mol. Cell* **14,** 657–666.
22. Hu, F., Alcasabas, A. A. & Elledge, S. J. (2001) *Genes Dev.* **15,** 1061–1066.
23. Emili, A., Schieltz, D. M., Yates, J. R., III, & Hartwell, L. H. (2001) *Mol. Cell* **7,** 13–20.
24. Smolka, M. B., Albuquerque, C. P., Chen, S. H., Schmidt, K. H., Wei, X. X., Kolodner, R. D. & Zhou, H. (2005) *Mol. Cell. Proteomics* **4,** 1358–1369.
25. Groth, A., Lukas, J., Nigg, E. A., Sillje, H. H., Wernstedt, C., Bartek, J. & Hansen, K. (2003) *EMBO J.* **22,** 1676–1687.
26. Carrera, P., Moshkin, Y. M., Gronke, S., Sillje, H. H., Nigg, E. A., Jackle, H. & Karch, F. (2003) *Genes Dev.* **17,** 2578–2590.
27. Desany, B. A., Alcasabas, A. A., Bachant, J. B. & Elledge, S. J. (1998) *Genes Dev.* **12,** 2956–2970.
28. Myung, K., Pennaneach, V., Kats, E. S. & Kolodner, R. D. (2003) *Proc. Natl. Acad. Sci. USA* **100,** 6640–6645.
29. Ramey, C. J., Howar, S., Adkins, M., Linger, J., Spicer, J. & Tyler, J. K. (2004) *Mol. Cell. Biol.* **24,** 10313–10327.
30. Linger, J. G. & Tyler, J. K. (2005) *Genetics* **171,** 1513–1522.
31. Lambert, S. & Carr, A. M. (2005) *Biochimie* **87,** 591–602.
32. Cobb, J. A., Shimada, K. & Gasser, S. M. (2004) *Curr. Opin. Genet. Dev.* **14,** 292–300.
33. Melo, J. A., Cohen, J. & Toczyski, D. P. (2001) *Genes Dev.* **15,** 2809–2821.
34. Allen, J. B., Zhou, Z., Siede, W., Friedberg, E. C. & Elledge, S. J. (1994) *Genes Dev.* **8,** 2401–2415.
35. Gardner, R., Putnam, C. W. & Weinert, T. (1999) *EMBO J.* **18,** 3173–3185.
36. Adkins, M. W. & Tyler, J. K. (2004) *J. Biol. Chem.* **279,** 52069–52074.
37. Franco, A. A., Lam, W. M., Burgers, P. M. & Kaufman, P. D. (2005) *Genes Dev.* **19,** 1365–1375.
38. Pulm, W. & Knippers, R. (1984) *Adv. Exp. Med. Biol.* **179,** 127–141.
39. Lopes, M., Cotta-Ramusino, C., Pellicioli, A., Liberi, G., Plevani, P., Muzi-Falconi, M., Newlon, C. S. & Foiani, M. (2001) *Nature* **412,** 557–561.
40. Lucca, C., Vanoli, F., Cotta-Ramusino, C., Pellicioli, A., Liberi, G., Haber, J. & Foiani, M. (2004) *Oncogene* **23,** 1206–1213.
41. Harkness, T. A., Arnason, T. G., Legrand, C., Pisclevich, M. G., Davies, G. F. & Turner, E. L. (2005) *Eukaryot. Cell* **4,** 673–684.
42. Sharp, J. A., Franco, A. A., Osley, M. A. & Kaufman, P. D. (2002) *Genes Dev.* **16,** 85–100.
43. Sharp, J. A., Krawitz, D. C., Gardner, K. A., Fox, C. A. & Kaufman, P. D. (2003) *Genes Dev.* **17,** 2356–2361.